



## Universality of phenotypic distributions in bacteria

Kuheli Biswas  and Naama Brenner 

Department of Chemical Engineering and Network Biology Research Laboratory,  
Technion - Israel Institute of Technology, Haifa 32000, Israel



(Received 25 March 2023; accepted 17 April 2024; published 17 May 2024)

Some phenotypic properties in bacteria exhibit universal statistics, with distributions collapsing under scaling. The extent and origins of such universality are not well understood. Using phenomenological modeling of growth and division, we identify compound “shape factors” that describe the distributions throughout a large set of single-cell data. We find that the emergence of universal distributions is associated with the robustness of shape factors across conditions, explaining the universality of cell size and highly expressed protein content and the nonuniversality of times between consecutive divisions. A wide range of experimental data sets support our theory quantitatively.

DOI: [10.1103/PhysRevResearch.6.L022043](https://doi.org/10.1103/PhysRevResearch.6.L022043)

**Introduction.** Bacterial growth and division have fascinated scientists and have been studied for decades. Mathematical models to account for the variability in cell size and interdivision times across time and among individuals were developed early on [1–4], but the comparison to data at the time was limited. More recent single-cell imaging and microfluidics technology yields high-quality data with large statistical power [5–12], enabling to test quantitative models of growth and division and the relation between temporal dynamics and statistical properties.

Previous works have reported that the distributions of cell size and highly expressed proteins are non-Gaussian, skewed and well approximated by a log-normal form [7,13–16]. These distributions have a universal shape, as manifested by their collapse under scaling [17,18]. In physics, such distribution collapse is associated with the insensitivity of macroscopic properties to underlying microscopic ones [19]. In biological systems, analogous collapse appears in different contexts, but its origin and extent are still not well understood [20–22]

The distribution of times between divisions has also been extensively studied, but here the emerging picture is less conclusive. Some experiments report a Gaussian-like distribution of division times [8,9,18,23], while others find more skewed distributions [1,2,12,24–26]. Some of these report a universal shape for division times [18,27]. Modeling work assuming a small-noise approximation has concluded that times between divisions are distributed approximately Gaussian [15]. In contrast, “sloppy size control” models [28] as well as other modeling approaches [29–31] find skewed distributions. Thus, a unifying framework that can explain the observed diversity and apparent disagreement in division time distribution shapes is lacking.

Here, we compute the division time distribution using stochastic threshold crossing techniques in a phenomenological coarse-grained model of growth and division. We find that the ratio between two stochastic parameters—variability in exponential growth rate and in threshold—defines a dimensionless “shape factor” that governs the distribution shape beyond shift and scale transformations. Analyzing a large set of single-cell data from microfluidic experiments, we find that division time distributions span a range of diverse behaviors, from almost Gaussian to very skewed. Our theoretical predictions, based on direct estimation of dynamic parameters, agree with the data throughout this range of behaviors. Combining these observations with known properties of cell size and highly expressed protein content, we address the question of universality. By observing the spread of data points in the landscape of shape factors, we find that for cell size and protein, the data adhere near a manifold of constant shape factor, while for division times they scatter through multiple contour lines. This finding sheds light on the universality of size and protein distributions, and likewise on the nonuniversality (or shape diversity) of division time distributions. It highlights the emergence of compound parameter combinations, whose sensitivity is key to understanding the system’s behavior.

**Model definition.** High-resolution single-cell measurements have revealed that in several bacterial species, cell size and content of highly expressed protein grow smoothly and exponentially across each cycle [8,25,26]; division occurs abruptly—consistent with the idea of triggering by some threshold event [Fig. 1(a)]. The growth dynamics during the  $n$ th cycle can thus be approximated as

$$x_n(t) = x_n^b e^{\alpha_n t} = x_n^b e^{\phi_n(t)}, \quad 0 < t < T_n. \quad (1)$$

Here  $x_n$  is the cell size (or highly expressed protein), with  $x_n^b$  the value at birth.  $\alpha_n$  the effective growth rate, and  $\phi_n(t)$  the Logarithmic Fold Change (LFC). The cycle ends at time  $t = T_n$  with symmetric division of both biomass and protein content. We formulate a generalized stochastic threshold-crossing model of division that unifies different previously studied models as special cases.

Published by the American Physical Society under the terms of the [Creative Commons Attribution 4.0 International license](https://creativecommons.org/licenses/by/4.0/). Further distribution of this work must maintain attribution to the author(s) and the published article’s title, journal citation, and DOI.

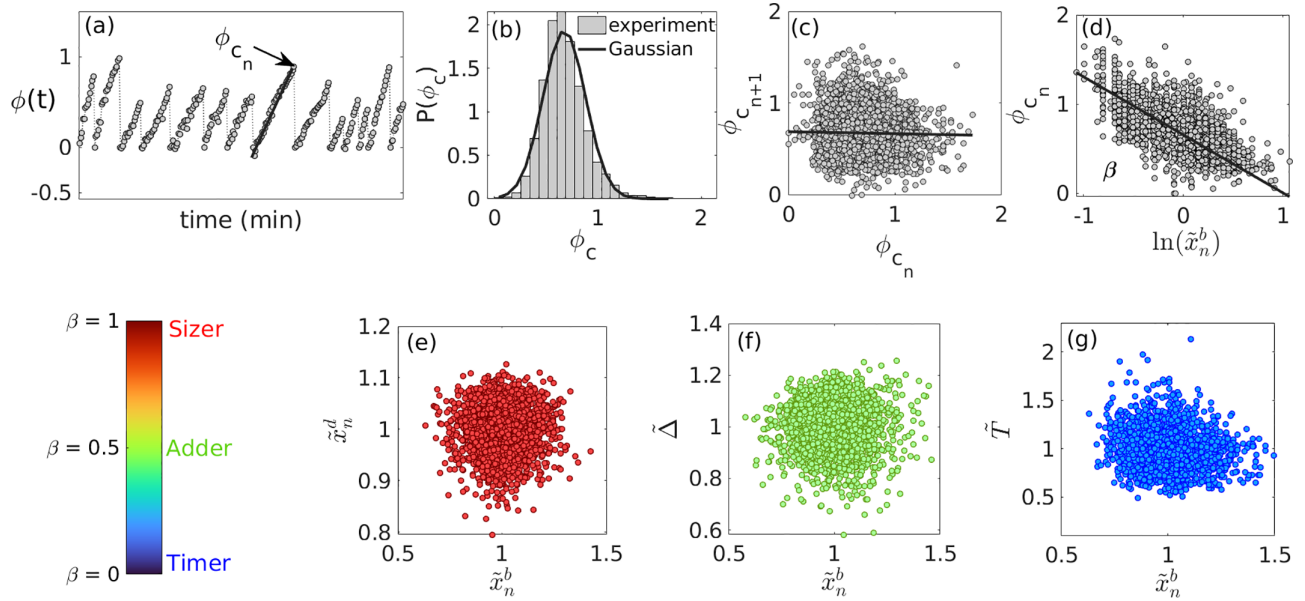


FIG. 1. Coarse-grained model of growth and based on statistical phenomenology. (a)–(d): Data from [26], where *E. coli* were grown in a microfluidic device. (a) Single *E. coli* bacteria grow exponentially; Logarithmic fold change (LFC) in cell size is linear within each cycle,  $\phi(t) = \alpha t$ . (b) At division, LFC reaches a stochastic threshold  $\phi_c$ , with distribution  $P(\phi_c)$  approximately Gaussian ( $\mu_\phi \approx \ln 2$ ,  $\sigma_\phi = 0.17$ ). (c) Across consecutive cycles,  $\phi_c$  are approximately independent. Correlation coefficient  $\approx -0.02$ . (d) The threshold  $\phi_c$  is negatively correlated with normalized birth size  $\tilde{x}_n$  with best-fit slope  $\beta = 0.65$ . (e)–(g) Scatter plots from simulations of the phenomenological model, Eqs. (1) and (2). Division size (e), added size (f), and cycle time (g) vs normalized initial size. The independence of these variables on initial condition is often interpreted as indicating a control mechanism where they are kept constant. By tuning the homeostasis parameter  $\beta$ , the model reduces to previously studied modes of division control: (e) sizer ( $\beta = 0.9$ ), (f) adder ( $\beta = 0.5$ ), and (g) approximate timer ( $\beta = 0.2$ ) as special cases.  $10^4$  generations were simulated with  $\alpha = 0.023 \text{ min}^{-1}$  and  $\xi = \mathcal{N}(0, 0.15)$ . See [32] for more details.

The LFC along the  $n$ th cycle is by definition zero at birth  $\phi_n(0)=0$ , and at division reaches a fluctuating value  $\phi_{c_n}$  [Fig. 1(a)]. These fluctuations are well described by a Gaussian distribution around  $\ln 2$  [Fig. 1(b)], approximately independent across cycles [Fig. 1(c)] and negatively correlated with the value at birth [Fig. 1(d)]. These statistical properties are well captured by the following phenomenological expression [25]

$$\phi_{c_n} = \ln 2 - \beta \ln(\tilde{x}_n^b) + \xi_n. \quad (2)$$

Here  $\xi_n$  is a Gaussian white noise with zero mean,  $\tilde{x}_n^b$  the birth size normalized by its mean, and  $0 < \beta \leq 1$  the slope of Fig. 1(d). Due to the log-normal distribution of size,  $\phi_c$  is a sum of two Gaussian variables, and therefore also Gaussian. The negative correlation induces a stable size distribution over multiple generations, interpolating between previously described division models [15,16,25,33,34]. To demonstrate this, we simulate the model in Eqs. (1) and (2) and present the resulting scatterplots of different variables vs initial cell size in Figs. 1(e)–1(g). Such plots have been extensively used to identify modes of division control. For example in Fig. 1(f), added size is independent of the birth size, a correlation known as the “adder” mode of division control. Sizer and timerlike correlations are found for other values of  $\beta$  in Figs. 1(e) and 1(g). The mathematical mapping between the current and previously formulated models is elaborated in [32].

*Model solution.* Equations (1) and (2) together constitute a phenomenological model that was successfully solved for cell size and protein distributions [15,16], and will be analyzed below in terms of division time statistics. We assume that cell division occurs when the LFC crosses a fluctuating threshold; this does not necessarily imply a mechanistic interpretation, but rather a tool for calculation. Using the threshold crossing formalism [35,36], we assume that cell division occurs when the stochastic process  $P(\phi_c) = \mathcal{N}(\ln 2, \sigma_\phi)$  crosses the absorbing boundary  $\phi(t) = \alpha t$  [37]. The survival probability—the probability that the cell has not divided till time  $t$ —can then be expressed as

$$S(t) = \int_{\phi(t)}^{\infty} P(\phi_c) d\phi_c = \frac{1}{2} \left[ 1 - \operatorname{erf} \left( \frac{\phi(t) - \ln 2}{\sqrt{2\sigma_\phi^2}} \right) \right]. \quad (3)$$

For a fixed growth rate  $\alpha$ , the probability density of  $S(t)$  will be

$$P(T|\alpha) = \frac{\alpha}{\sqrt{2\pi\sigma_\phi^2}} \exp \left[ -\frac{(\alpha T - \ln 2)^2}{2\sigma_\phi^2} \right]. \quad (4)$$

To incorporate the variability in growth rate across cycles,  $P(\alpha) = \mathcal{N}(\mu_\alpha, \sigma_\alpha)$  [Fig. 2(a)], we integrate Eq. (4) with  $P(\alpha)$ ,

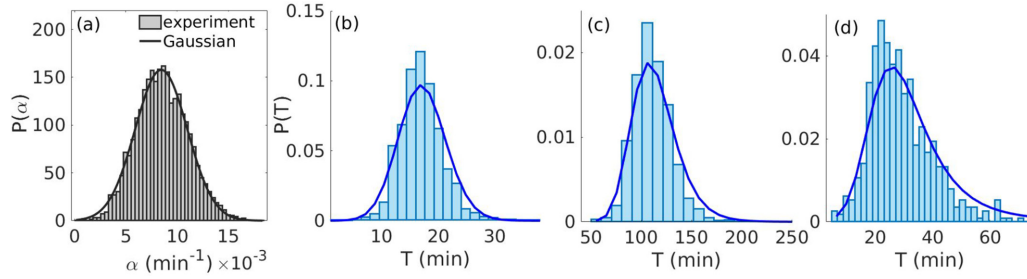


FIG. 2. Experimental division time distributions are predicted across a range of shape factors. (a) Growth rates  $\alpha_n$ , obtained from the slope of  $\phi_n(t)$  [Fig. 1(a)] follow a Gaussian distribution,  $P(\alpha) = \mathcal{N}(\mu_\alpha, \sigma_\alpha)$ . In this experiment (data from [26]),  $\chi_\alpha = \sigma_\alpha/\mu_\alpha = 0.27$ . Other experiments show similarly Gaussian growth rate distributions, but with different  $\sigma_\alpha$ . (b)–(d) Division time distributions from different experiments (bars), corresponding to different shape factors  $\Sigma_T = \chi_\alpha/\sigma_\phi$ , are well predicted by theoretical result Eq. (5) (solid lines). The shape factors are (b)  $\Sigma_T = 0.64$  ([8], glucose medium), (c)  $\Sigma_T = 1.3$  ([11], arginine medium), and (d)  $\Sigma_T = 1.8$  ([25], LAC-M9 medium). In all experiments, *E. coli* bacteria were grown in mother machines; see details in [32].

yielding to the division time distribution [32]

$$P(T) = \int P(T|\alpha)P(\alpha)d\alpha = \frac{(\mu_\alpha\sigma_\phi^2 + \sigma_\alpha^2T \ln 2)}{\sqrt{2\pi}(\sigma_\phi^2 + (\sigma_\alpha T)^2)^{3/2}} \exp\left[-\frac{(\mu_\alpha T - \ln 2)^2}{2(\sigma_\phi^2 + (T\sigma_\alpha)^2)}\right]. \quad (5)$$

Transforming this expression to dimensionless time [32], we find that it contains two dimensionless parameters:  $\sigma_\phi$ , a measure of threshold fluctuations, and  $\chi_\alpha = \sigma_\alpha/\mu_\alpha$ , a measure of growth-rate fluctuations. The shape of the distribution is strongly influenced by the ratio of these two parameters, which reflects the relative strength of the two noise sources in the model:  $\Sigma_T = \chi_\alpha/\sigma_\phi$ . We term this ratio the shape factor; it defines regions where the distribution resembles a Gaussian shape when  $\Sigma_T < 1$ , and a skewed heavy-tailed shape when  $\Sigma_T > 1$ .

Figures 2(b)–2(d) show a few examples taken from different experiments, illustrating a range of shape factors from  $\Sigma_T = 0.64$ , an almost Gaussian shape, to a larger value of  $\Sigma_T = 1.8$ , where the shape is skewed. The experimental data (bars) are well described by Eq. (5) (lines) throughout this range of behaviors. A larger collection of division time distributions can be seen in [32], all in good agreement with the theory. To quantify the alignment of our theoretical model with single-cell data, we conducted a Kolmogorov-Smirnov (KS) test, the results of which are detailed in Table II of the Supplemental Material [32]. Note that we have not employed a fitting procedure; to obtain the theoretical lines, we estimate stochastic variables  $\mu_\alpha$ ,  $\sigma_\alpha$ , and  $\sigma_\phi$  directly from dynamic trajectories such as those in Fig. 1(a). These are then inserted into Eq. (5).

*Universal and nonuniversal distributions.* The stochastic LFC threshold model was used in previous work to predict a log-normal distribution of cell size and protein content; its shape depends on the compound shape factor  $\Sigma_x = \sigma_\phi/\sqrt{\beta(2-\beta)}$ , which in turn depends on the threshold standard deviation  $\sigma_\phi$  and the homeostasis parameter  $\beta$  [15,16]. Here we identified the compound parameter  $\Sigma_T = \sigma_\phi/\chi_\alpha$  as determining the shape of the division time distribution. In contrast to the broad range of distribution shapes found for division time, cell size and highly expressed protein content were consistently reported to exhibit a universal

distribution shape [14,15,17,18,27]. We next investigate properties of the shape factors to shed light on the origins of universal distribution collapse.

In Figs. 3(a) and 3(b) we assemble data from a large set of single-cell experiments in the planes of stochastic parameters  $(\chi_\alpha, \sigma_\phi)$  and  $(\beta, \sigma_\phi)$ , respectively. Each point represents one experiment, where single-cell traces were pooled for estimation. In all cases, bacteria were grown in mother machines, but relevant conditions such as medium or temperature, as well as bacterial strain, vary among experiments (see Table 1 in [32]). In these parameter planes, the shape factor for division time (a) and cell size (b) are depicted as gray contour lines of constant values. Examining the embedding of data across the shape landscape reveals an important difference between the two phenotypes.

In (a), the data scatter across many contour lines, spanning a broad range of shape-factor values ( $\Sigma_T \sim 0.1$  to 3). Contributing to this variability is the broad range of growth rate noise  $\chi_\alpha$  ( $x$  axis; 0.05 to 0.5), to which the shape factor is inversely proportional. This is consistent with the broad range of behaviors we observed for division time distributions across data sets. Two examples of scaled distributions are shown in panel (c). In (b), in marked contrast, the data are concentrated in a small region around a single contour line, maintaining a constrained shape factor for cell size ( $\Sigma_x \approx 0.2$ ). The shape of the log-normal distribution is very weakly sensitive to the shape-parameter value in this regime [16]; together these properties lead to the collapse of these distributions upon scaling [panel (d)].

*Discussion.* We examined single-cell statistical properties using a phenomenological growth and division model. This model relies on several key assumptions: exponential growth during the cell cycle, variable exponential rates in successive cycles, and symmetric division triggered by a noisy threshold in log fold change of cell size—negatively correlated with birth size. This approach had been validated in previous

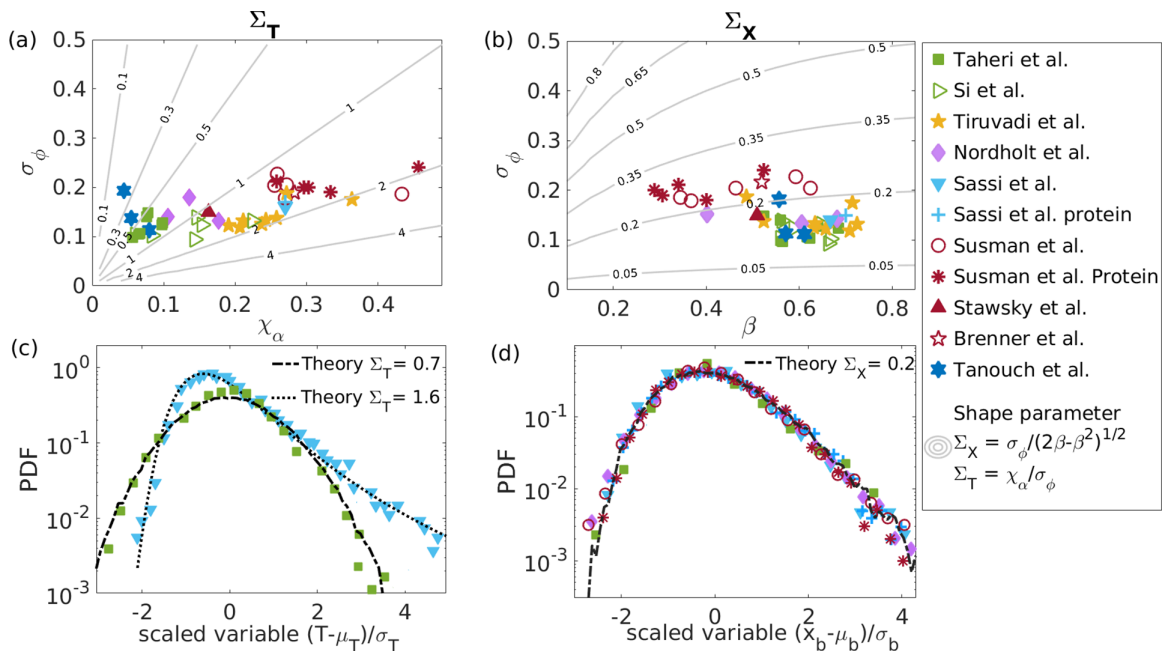


FIG. 3. (a) Plot of  $\chi_\alpha$  vs  $\sigma_\phi$ , estimated from experimental data (colored symbols), span a broad range of shape factors  $\Sigma_T$  (gray contours). (b) Plot of  $\sigma_\phi$  vs  $\beta$ , estimated for the same data, cluster around a small range of shape factor for cell size or protein  $\Sigma_X$  (gray contours). (c) The scaled distribution of cell division times is nonuniversal, showing a Gaussian-like distribution for  $\Sigma_T < 1$  (green squares, [8]) and a skewed shape for  $\Sigma_T > 1$  (blue triangles, [26]). The black curves are obtained from our theory Eq. (5). (d) The scaled distribution of cell size and protein number collapse under two-parameter scaling, and agree well with the theoretically predicted log-normal distribution (black curve). Data are taken from [7–12,23,25,26,38], see Table I of [32].

studies and encompasses various homeostasis modes, including adder, sizer, and timer scenarios as specific instances. Such a coarse-grained modeling approach, with few microscopic assumptions, allows us to explore general questions inspired by statistical physics—namely, universality of distributions and scaling phenomena. While such an approach has been used extensively, other more microscopic models have also been developed [39].

By employing a stochastic threshold crossing framework, we computed the distribution of division times. The approximations made in obtaining this result do not hinge on a small-noise approximation in growth rate across cell cycles (see [32]). In the data we analyzed, encompassing a wide spectrum of experiments in microfluidic traps, the small-noise limit only applies to a minority of experiments. The range of observed behaviors—from very narrow to very broad growth rate distribution—served as a central motivation for extending the phenomenological theory in our present study.

The resulting distribution has strictly no finite moments, but a limited range of data allows for a good comparison with an appropriate cutoff. Notably, this result accurately predicts the relationships between data moments and model parameters, as shown in [32]. The long tails of the distribution result from the Gaussian assumption for growth rates, tending to a reciprocal-Gaussian in the limit. Alternative assumptions, such as a Gamma distribution, yield empirically similar distributions [32], but do not provide an analytic expression that allows for identifying parameter dependencies and a clearly understandable shape factor.

Interestingly, the reciprocal-Gaussian distribution for generation times was tested as an empirical fit to division time statistics, and was found to be more suitable than the log-normal distribution [29].

The shape factor  $\Sigma_T$  governs the distribution shape beyond shift and scale, eliminated by two-parameter scaling. An analogous factor had previously been found for cell size, but its empirical values and significance for distribution scaling were not studied. By comparing the two shape factors we were able to illuminate the sources of distribution universality, as stemming from the robustness of these parameter combinations as experimental conditions are varied. This explanation remains phenomenological and does not clarify the source of difference in robustness. In particular, the reasons behind different levels of variability in single-cell growth rates among experimental conditions remain to be understood. It can be speculated that the sensitivity of growth rates to their environment and their strong correlation with division times over long timescales [38] make them effective control variables that allow flexibility for compensation. On the other hand, cell size does not partake in long-term homeostatic correlations; stable growth can occur at various cell sizes, rendering it an “irrelevant variable” in the sense of statistical mechanics with a universal distribution. These hypotheses warrant further investigation.

The description of cell size and highly expressed proteins has converged to a similar modeling framework. Both quantities adhere to the fundamental model assumptions outlined above; their dynamic variables (e.g.,  $\alpha_n$ ), which fluctuate across cycles, are strongly correlated with one another



on a cycle-by-cycle basis [7,25,26]. Consequently, in Fig. 3 we found that they share the same universal distribution shape. Intriguingly, the statistics of division time can be predicted based on the dynamics of either cell size or any highly expressed protein, with similar predictive success [32]. Thus, while cell division is likely triggered by multiple events, their tight interconnection reduces the complexity of the problem, allowing several options to predict statistical properties effectively. This aligns with previous observations of balanced exponential growth as a dynamic attractor characterized by robust relationships among constituents [31]. Understanding such reduction of effective dimensionality in high-dimensional yet highly correlated

systems like the biological cell remains an important open question.

*Acknowledgments.* K.B. is supported by a fellowship from the Lady Davis Foundation at the Technion. The research is supported in part by the Israeli Science Foundation (Grant No. 155/18), and the Binational Science Foundation (Grant No. 2016376). We are grateful to Erez Braun, Hanna Salman, Ariel Amir, and Ron Teichner for comments on the manuscript.

While preparing this work, the authors used ChatGPT to improve the readability and language of the work. After using this tool, we reviewed and edited the content as needed and take full responsibility for the paper's content.

- 
- [1] A. Koch and M. Schaechter, A model for statistics of the cell division process, *Microbiology* **29**, 435 (1962).
- [2] E. Powell and F. Errington, Generation times of individual bacteria: some corroborative measurements, *Microbiology* **31**, 315 (1963).
- [3] A. G. Marr, R. Harvey, and W. Trentini, Growth and division of *Escherichia coli*, *J. Bacteriol.* **91**, 2388 (1966).
- [4] W. Voorn and L. Koppes, Skew or third moment of bacterial generation times, *Arch. Microbiol.* **169**, 43 (1997).
- [5] F. Wu and C. Dekker, Nanofabricated structures and microfluidic devices for bacteria: from techniques to biology, *Chem. Soc. Rev.* **45**, 268 (2016).
- [6] P. Wang, L. Robert, J. Pelletier, W. L. Dang, F. Taddei, A. Wright, and S. Jun, Robust growth of *Escherichia coli*, *Curr. Biol.* **20**, 1099 (2010).
- [7] N. Brenner, E. Braun, A. Yoney, L. Susman, J. Rotella, and H. Salman, Single-cell protein dynamics reproduce universal fluctuations in cell populations, *Eur. Phys. J. E* **38**, 102 (2015).
- [8] S. Taheri-Araghi, S. Bradde, J. T. Sauls, N. S. Hill, P. A. Levin, J. Paulsson, M. Vergassola, and S. Jun, Cell-size control and homeostasis in bacteria, *Curr. Biol.* **25**, 385 (2015).
- [9] Y. Tanouchi, A. Pai, H. Park, S. Huang, R. Stamatov, N. E. Buchler, and L. You, A noisy linear map underlies oscillations in cell size and gene expression in bacteria, *Nature (London)* **523**, 357 (2015).
- [10] D. Yang, A. D. Jennings, E. Borrego, S. T. Retterer, and J. Männik, Analysis of factors limiting bacterial growth in PDMS mother machine devices, *Front. Microbiol.* **9**, 871 (2018).
- [11] F. Si, G. Le Treut, J. T. Sauls, S. Vadia, P. A. Levin, and S. Jun, Mechanistic origin of cell-size control and homeostasis in bacteria, *Curr. Biol.* **29**, 1760 (2019).
- [12] S. Tiruvadi-Krishnan, J. Männik, P. Kar, J. Lin, A. Amir, and J. Männik, Coupling between DNA replication, segregation, and the onset of constriction in *Escherichia coli*, *Cell Rep.* **38**, 110539 (2022).
- [13] C. Furusawa, T. Suzuki, A. Kashiwagi, T. Yomo, and K. Kaneko, Ubiquity of log-normal distributions in intra-cellular reaction dynamics, *Biophysics* **1**, 25 (2005).
- [14] K. Hosoda, T. Matsuura, H. Suzuki, and T. Yomo, Origin of lognormal-like distributions with a common width in a growth and division process, *Phys. Rev. E* **83**, 031118 (2011).
- [15] A. Amir, Cell size regulation in bacteria, *Phys. Rev. Lett.* **112**, 208102 (2014).
- [16] N. Brenner, C. M. Newman, D. Osmanović, Y. Rabin, H. Salman, and D. L. Stein, Universal protein distributions in a model of cell growth and division, *Phys. Rev. E* **92**, 042713 (2015).
- [17] H. Salman, N. Brenner, C. K. Tung, N. Elyahu, E. Stolovicki, L. Moore, A. Libchaber, and E. Braun, Universal protein fluctuations in populations of microorganisms, *Phys. Rev. Lett.* **108**, 238105 (2012).
- [18] S. Iyer-Biswas, C. S. Wright, J. T. Henry, K. Lo, S. Burov, Y. Lin, G. E. Crooks, S. Crosson, A. R. Dinner, and N. F. Scherer, Scaling laws governing stochastic growth and division of single bacterial cells, *Proc. Natl. Acad. Sci. USA* **111**, 15912 (2014).
- [19] A. Cohen, Y. Roth, and B. Shapiro, Universal distributions and scaling in disordered systems, *Phys. Rev. B* **38**, 12125 (1988).
- [20] L.-h. So, A. Ghosh, C. Zong, L. A. Sepúlveda, R. Segev, and I. Golding, General properties of transcriptional time series in *Escherichia coli*, *Nat. Genet.* **43**, 554 (2011).
- [21] H.-Y. Shih, H. Mickalide, D. T. Fraebel, N. Goldenfeld, and S. Kuehn, Biophysical constraints determine the selection of phenotypic fluctuations during directed evolution, *Phys. Biol.* **15**, 065003 (2018).
- [22] O. Agam and E. Braun, Universal calcium fluctuations in hydra morphogenesis, *Phys. Biol.* **20**, 066002 (2023).
- [23] N. Nordholt, J. H. van Heerden, and F. J. Bruggeman, Biphasic cell-size and growth-rate homeostasis by single *Bacillus subtilis* cells, *Curr. Biol.* **30**, 2238 (2020).
- [24] J. L. Lebowitz and S. Rubinow, A theory for the age and generation time distribution of a microbial population, *J. Math. Biol.* **1**, 17 (1974).
- [25] L. Susman, M. Kohram, H. Vashistha, J. T. Nechleba, H. Salman, and N. Brenner, Individuality and slow dynamics in bacterial growth homeostasis, *Proc. Natl. Acad. Sci. USA* **115**, E5679 (2018).
- [26] A. S. Sassi, M. Garcia-Alcala, M. Aldana, and Y. Tu, Protein concentration fluctuations in the high expression regime: Taylor's law and its mechanistic origin, *Phys. Rev. X* **12**, 011051 (2022).
- [27] A. S. Kennard, M. Osella, A. Javer, J. Grilli, P. Nghe, S. J. Tans, P. Cicuta, and M. Cosentino Lagomarsino, Individuality and universality in the growth-division laws of single *E. coli* cells, *Phys. Rev. E* **93**, 012408 (2016).
- [28] J. J. Tyson and O. Diekmann, Sloppy size control of the cell division cycle, *J. Theor. Biol.* **118**, 405 (1986).

- [29] H. Kubitschek, The distribution of cell generation times, *Cell Proliferation* **4**, 113 (1971).
- [30] R. Pugatch, Greedy scheduling of cellular self-replication leads to optimal doubling times with a log-frechet distribution, *Proc. Natl. Acad. Sci. USA* **112**, 2611 (2015).
- [31] P. P. Pandey, H. Singh, and S. Jain, Exponential trajectories, cell size fluctuations, and the adder property in bacteria follow from simple chemical dynamics and division control, *Phys. Rev. E* **101**, 062406 (2020).
- [32] See Supplemental Material at <http://link.aps.org/supplemental/10.1103/PhysRevResearch.6.L022043> for contains details of the model, the analytic calculations and approximations involved, information on the data used for analysis and more extended analyses of these data.
- [33] D. A. Kessler and S. Burov, Effective potential for cellular size control, [arXiv:1701.01725](https://arxiv.org/abs/1701.01725).
- [34] P.-Y. Ho, J. Lin, and A. Amir, Modeling cell size regulation: From single-cell-level statistics to molecular mechanisms and population-level effects, *Annu. Rev. Biophys.* **47**, 251 (2018).
- [35] C. W. Gardiner, *Handbook of Stochastic Methods* (Springer, Berlin, 1985), Vol. 3.
- [36] H. Risken, Fokker-planck equation, *The Fokker-Planck Equation* (Springer, 1996) pp. 63–95.
- [37] L. Luo, Y. Bai, and X. Fu, Stochastic threshold in cell size control, *Phys. Rev. Res.* **5**, 013173 (2023).
- [38] A. Stawsky, H. Vashistha, H. Salman, and N. Brenner, Multiple timescales in bacterial growth homeostasis, *iScience* **25**, 103678 (2022).
- [39] C. Jia, A. Singh, and R. Grima, Cell size distribution of lineage data: analytic results and parameter inference, *iscience* **24**, 102220 (2021).